Optically thin terahertz metamaterials

Ranjan Singh,[1] Evgenya Smirnova,[2] Antoinette J. Taylor,[3] John F. O'Hara,[3] and Weili Zhang[1,*]

[1]*School of Electrical and Computer Engineering, Oklahoma State University, Stillwater, Oklahoma 74078, USA*
[2]*ISR-6, Los Alamos National Laboratory, P.O. Box 1663, MS H851, Los Alamos, NM 87545, USA*
[3]*MPA-CINT, Los Alamos National Laboratory, P.O. Box 1663, MS K771, Los Alamos, NM 87545, USA*
[*]*Corresponding author: weili.zhang@okstate.edu*

Abstract: Resonant properties of optically thin metamaterials are studied by terahertz time-domain spectroscopy. Both the lower energy inductor-capacitor (LC) and the higher energy dipole resonances of the planar double split-ring resonators (SRRs) exhibit characteristic evolution with various sub-skin-depth thicknesses of the constituent Pb film. The signature of the LC resonance begins to emerge at a critical thickness near 0.15 skin depth. The resonances reveal a characteristic enhancement; they are strengthened remarkably with increasing SRR thicknesses at sub-skin-depth level and then gradually saturate beyond the skin depth.

OCIS codes: (300.6495) Spectroscopy, terahertz; (160.3918) Metamaterials

References and links

1. V. G. Veselago, "The Electrodynamics of Substances with Simultaneously Negative Values of ε and μ,"Sov. Phys. Usp. **10**, 509 (1968).
2. D. R. Smith, W. J. Padilla, D. C. Vier , S. C. Nemat-Nasser, S. Schultz, "Composite Medium with Simultaneously Negative Permeability and Permittivity," Phys. Rev. Lett. **84**, 184 (2000).
3. J. B. Pendry, A. Holden, D. Robbins, W. Stewart, "Magnetism from conductors and enhanced nonlinear phenomena," IEEE Trans. Microwave Theory Tech. **7**, 2075 (1999).
4. S. Zhang, W. Fan, N. C. Panoiu, K. J. Malloy, R. M. Osgood, and S. R. J. Brueck, "Experimental demonstration of near-infrared negative-index metamaterials," Phys. Rev. Lett. **95**, 137404 (2005).
5. T. J. Yen, W. J. Padilla, N. Fang, D. C. Vier, D. R. Smith, J. B. Pendry, D. N. Basov, and X. Zhang, "Terahertz magnetic response from artificial materials," Science **303**, 1494 (2004).
6. S. Linden, C. Enkrich, M. Wegener, J. Zhou, T. Koschny, and C. M. Soukolis, "Magnetic response of metamaterials at 100 Terahertz," Science **306**, 1351 (2004).
7. N. Katsarakis, G. Konstantinidis, A. Kostopoulos, R. S. Penciu, T. F. Gundogdu, M. Kafesaki, E. N. Economou, T. Koschny, and C. M. Soukoulis, "Magnetic response of split-ring resonators in the far-infrared frequency regime," Opt. Lett. **30**, 1348 (2005).
8. A. K. Azad, J. M. Dai, and W. Zhang, "Transmission properties of terahertz pulses through subwavelength double split-ring resonators," Opt. Lett. **31**, 634 (2006).
9. W. J. Padilla, A. J. Taylor, C. Highstrete, M. Lee, and R. D. Averitt, "Dynamical electric and magnetic metamaterial response at terahertz frequencies," Phys. Rev. Lett. **96**, 107401 (2006).
10. H.-T. Chen, W. J. Padilla, J. M. O. Zide, A. C. Gossard, A. J. Taylor, and R. D. Averitt, "Active terahertz metamaterial devices," Nature, **444**, 597 (2006).
11. T. Driscoll, G. O. Andreev, D. N. Basov, S. Palit, S. Y. Cho, N. M. Jokerst, and D. R. Smith, "Tuned permeability in terahertz split-ring resonators for devices and sensors," Appl. Phys. Lett. **91**, 062511 (2007).
12. C. Debus and P. H. Bolivar, "Frequency selective surfaces for high sensitivity terahertz sensing," Appl. Phys. Lett. **91**, 184102 (2007).
13. J. F. O'Hara, R. Singh, I. Brener, E. Smirnova, J. Han, A. J. Taylor, and W. Zhang, "Thin-film sensing with planar terahertz metamaterials: sensitivity and limitations," Opt. Express **16**, 1786 (2008).
14. N. Wongkasem, A. Akyurtlu, J. Li, A. Tibolt, Z. Kang, and W. D. Goodhue, "Novel broadband terahertz negative refractive index metamaterials: analysis and experiment," Progress In Electromagnetic Research, PIER **64**, 205 (2006).
15. H.-T. Chen, J. F. O' Hara, A. J. Taylor, and R. D. Averitt, "Complementary planar terahertz metamaterials," Opt. Express **15**, 1084 (2007).
16. S. Ramo and J. R. Whinnery, *Fields and waves in Modern Radio*, (Wiley, New York, 1953), Chap. 6, p. 239.
17. A. K. Azad and W. Zhang, "Resonant terahertz transmission in subwavelength metallic hole arrays of sub-skin-depth thickness," Opt. Lett. **30**, 2945 (2005).
18. M. A Ordal , L. L. Long, R. J. Bell, S. E. Bell, R. R. Bell, R. W. Alexander, Jr., and C. A Ward, "Optical properties of the metals Al, Co, Cu, Au, Fe, Pb, Ni, Pd, Pt, Ag, Ti, and W in the infrared and far infrared," Appl. Opt. **22**, 1099 (1983).

#94061 - $15.00 USD Received 19 Mar 2008; revised 21 Apr 2008; accepted 21 Apr 2008; published 23 Apr 2008

19. D. Grischkowsky, S. Keiding, M. van Exter, and Ch. Fattinger, "Far-infrared time-domain spectroscopy with terahertz beams of dielectrics and semiconductors," J. Opt. Soc. Am. B **7**, 2006 (1990).
20. R. Marques, F. Mesa, J. Martel, and F. Median, "Comparative analysis of edge- and broadside- coupled split ring resonators for metamaterial design-theory and experiments," IEEE Trans. on Antennas and Propag. **51**, 2572 (2003).
21. J. F. O'Hara, E. Smirnova, A. K. Azad, H.-T. Chen, and A. J. Taylor, "Effects of microstructure variations on macroscopic terahertz metafilm properties," Active and Passive Electronic Components **2007**, 49691 (2007).
22. J. W. C. De Vries, "Temperature and thickness dependence of the resistivity of thin polycrystalline aluminum, cobalt, nickel, palladium, silver and gold films," Thin Solid Films **167**, 25 (1988).
23. N. Laman and D. Grischkowsky, "Reduced conductivity in the terahertz skin-depth layer of metals," Appl. Phys. Lett. **90**, 122115 (2007).
24. M. Walther, D. G. Cooke, C. Sherstan, M. Hajar, M. R. Freeman, and F. A. Hegmann, "Terahertz conductivity of thin gold films at the metal-insulator percolation transition" Phys. Rev. B **76**, 125408 (2007).
25. CST Microwave Studio ®, © 2008 CST - Computer Simulation Technology, Wellesley Hills, MA, USA, www.cst.com.

1. Introduction

Controlling the electromagnetic response of materials through structural tailoring on the subwavelength scale has recently attracted much attention, and plenty of research has been focused on exploring the resulting extraordinary electromagnetic phenomena. These deliberately designed structures have electromagnetic responses that give rise to fascinating effects such as artificial magnetism and negative refraction, and are known as metamaterials [1-4]. Electromagnetic metamaterials are composite structures having inclusions smaller than the wavelength of incident electromagnetic waves so that the waves encounter an effectively homogeneous medium. It has been shown that artificial magnetic materials can be made available at terahertz frequencies from non-magnetic materials such as metallic split-ring resonators (SRRs) [5, 6]. It has also been found that an SRR exhibits a strong electric resonance at normal wave incidence at the same frequency as the magnetic resonance [7-15].

Recently, several techniques have been demonstrated with the capability of modifying the electromagnetic response of metamaterials. The modification is either in the form of resonance frequency shifting or resonance amplitude modulation [9-13]. In the terahertz regime, the resonance strength of planar metamaterials can be actively controlled by either photoexciting the free carriers in the substrate at the capacitor gap or supplying external voltage to a hybrid structure consisting of Schottky diodes integrated into a planar metamaterial [9,10]. So far, metamaterials in a broad spectral range have employed metallic structures of above-skin-depth thickness and can be referred to as optically thick metamaterials. It is interesting to explore the resonance behavior of metamaterials with sub-skin-depth thickness. In this article, we present optically thin metamaterials that have the capability to respond to freely propagating terahertz pulses by use of planar double SRRs made from Pb films with thicknesses below the skin depth, δ. Terahertz time-domain spectroscopy (THz-TDS) measurements indicate that a 0.1δ (34 nm) thick SRR array is nearly transparent to the normally incident terahertz pulses, whereas the 0.15δ (50 nm) thick SRRs attenuate the amplitude by 35%, reshape the transmitted terahertz pulses, and begin to reveal signatures of the inductor-capacitor (LC) and dipole resonances at 0.5 and 1.6 THz, respectively. The enhancement in the LC resonance shows a characteristic behavior with SRR thicknesses on the sub-skin-depth scale and saturates beyond one skin depth.

Skin depth is defined as the penetration depth of electromagnetic waves in a conductor at which the field amplitude decreases, normally to the surface, to 1/e of its value at the surface. The skin depth for metals is calculated using $\delta = 1/\sqrt{\pi f \mu_0 \sigma_{dc}}$ [16], where f is the frequency at which the skin depth is defined, μ_0 is the vacuum permeability, and σ_{dc} is the d.c. conductivity of metal. The calculated skin depths for Pb, Al, and Ag at the LC resonance frequency 0.5 THz are δ = 336, 116, and 84 nm, respectively [17,18]. Here, Pb is chosen as the constituent metal for optically thin SRRs because of its large value of skin depth. This allows for a remarkable dynamic range in characterizing the resonance evolution with various

#94061 - $15.00 USD Received 19 Mar 2008; revised 21 Apr 2008; accepted 21 Apr 2008; published 23 Apr 2008

sub-skin-depth thicknesses. In addition, Pb behaves as a good conductor at terahertz frequencies with a high complex conductivity $\sigma = 4.5\times10^{6} + i4.9\times10^{4}\,\Omega^{-1}\mathrm{m}^{-1}$ at 0.5 THz [17,18], which facilitates establishing the well-defined LC and dipole resonances in the SRR metamaterials.

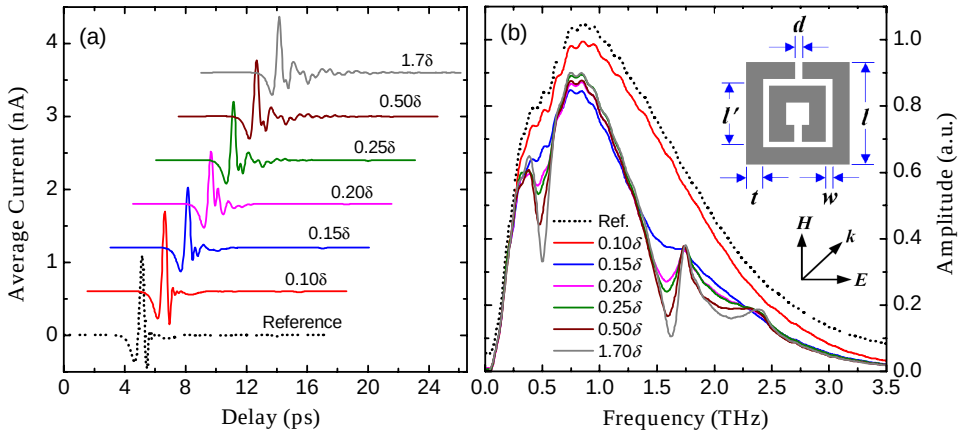

Fig. 1. (a). Transmitted terahertz pulses through the reference and Pb SRR metamaterials of different thicknesses. For clarity, the curves are shifted by 1.5 ps in time and 0.6 nA in average current. (b) Corresponding Fourier transformed spectra that illustrate the evolution of the resonances. The E-field of the terahertz pulses is perpendicular to the SRR gaps. The reference is shifted up by 0.05 for clarity. Inset: schematic diagram of the double SRRs.

2. Experiments

A set of Pb SRR arrays of various thicknesses, ranging from 0.1δ to 1.7δ (571 nm) is fabricated by conventional photolithography processing on a silicon substrate (0.64-mm-thick, p-type resistivity 20 Ω cm). The inset of Fig. 1 shows a diagram of the double SRR with a minimum feature d = 2 μm in the splits of the rings and other dimensions of w = 3 μm, t = 6 μm, l = 36 μm, and a lattice constant P = 50 μm. Each SRR array has a 20 mm × 20 mm clear aperture. The SRR metamaterials are characterized by THz-TDS in a broadband, photoconductive switch based system that consists of four parabolic mirrors in an 8-F confocal geometry [8,19]. The orientation of SRRs is such that the terahertz electric field is perpendicular to the splits in the rings, as shown in the inset of Fig. 1. The SRR array is placed at the waist of the 3.5-mm-diameter, frequency-independent focused beam, and the terahertz radiation penetrates the SRRs at normal incidence.

Figure 1(a) shows an evolution of the terahertz pulses transmitted through a reference and the SRR arrays of various thicknesses, and the corresponding Fourier transformed amplitude spectra are illustrated in Fig. 1(b). The reference is a blank silicon slab identical to the SRR substrate. The transmitted terahertz pulses as well as the spectrum for the 0.1δ thick SRRs appear nearly identical to the reference, showing that such a thin SRR is almost transparent to the incident terahertz pulses. However, when the SRR thickness is increased to 0.15δ, a 35% peak-to-peak attenuation and a reshaping of the pulse in the time domain is clearly observed. A further 25% peak-to-peak attenuation also occurs by increasing the thickness to 0.2δ. Also, an adjoining feature along with the main pulse is revealed, which becomes most distinguished for the 0.2δ thick SRRs and then gradually disappears with thicker Pb films. In the frequency

#94061 - $15.00 USD Received 19 Mar 2008; revised 21 Apr 2008; accepted 21 Apr 2008; published 23 Apr 2008

domain, three distinct resonances are developed as transmission dips with increasing SRR thickness. They are the LC resonance, ω_{LC} at 0.5 THz, the electric dipole resonance, ω_0 at 1.6 THz, and a weaker electric quadrupole resonance near 2.0 THz. The LC resonance is due to inductive currents circulating around the ring perimeter in conjunction with capacitive charge accumulation at the ring gaps. In contrast, the dipole and higher resonances are due to antenna-like couplings between the SRR conductors parallel to the E-field. The signature of the LC resonance begins to show up with the 0.15δ thick SRRs, while it sharpens to a greater extent with the 0.2δ thick SRRs. Thus, a critical thickness exists near 0.15δ that is required to excite the LC resonance for the Pb film. A further reshaping of the terahertz pulses and the corresponding strengthening of resonances in the spectra occur with higher SRR thicknesses.

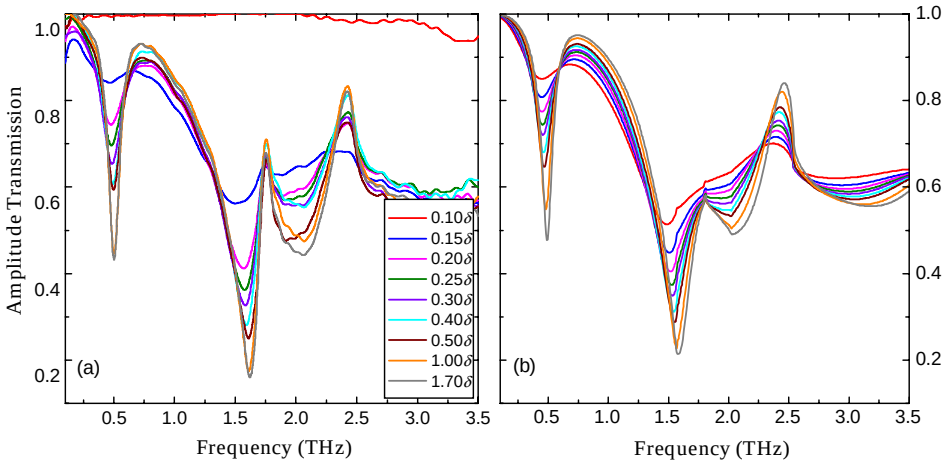

Fig. 2. (a). Frequency dependent amplitude transmission of the SRR metamaterials with various thicknesses of Pb film. (b) Corresponding simulation result by CST Microwave Studio.

Figure 2(a) shows the frequency dependent amplitude transmission of the SRRs with various thicknesses. The transmission is extracted from the ratio of the Fourier-transformed amplitude spectra of the samples to the reference [8]. With an increasing metal thickness from 0.1 to 1.0δ, the LC resonance exhibits extensive evolution, and then it is nearly stabilized when the SRR thickness is beyond 1.0δ. The transmission minimum at the LC resonance is shown in Fig. 3(a) as a function of metal thickness in terms of skin depth. The resonance minimum is strengthened from ~1.0 to 0.43 with increasing sub-skin-depth metal thickness, while it tends to saturate when the SRRs are thicker than a skin depth.

3. Discussion

3.1 Analysis of experimental results

The behavior of the main Lorentzian resonance in SRRs is well-known and follows the form of a series RLC circuit. The inductance, *L*, in the circuit results from current circulating around the SRR perimeter, while the capacitance, *C*, is due to charge accumulation at the gaps. For double SRRs there is an additional capacitive contribution between the two rings. A higher circulating current should result in a stronger resonance. The resistance of the metallic SRRs is directly correlated to the circulating current, and plays a very important role in making these subwavelength structures highly resonant [3, 10, 20]. The decrease in effective

#94061 - $15.00 USD Received 19 Mar 2008; revised 21 Apr 2008; accepted 21 Apr 2008; published 23 Apr 2008

resistance R of the SRRs is mainly responsible for the enhanced LC resonance with increasing sub-skin-depth thickness. The effective resistance of the SRRs can be estimated by the equivalent ring model for current distribution [20]. For the square double SRRs, the effective resistance is approximately given as $R = 4l'/(th\sigma)$ with $h < 2\delta$ and $R = 2l'/(t\delta\sigma)$ for $h \geq 2\delta$, where l' = 21 μm is the average side length of the SRRs, t is the width of the metal lines, and h and σ being the thickness and conductivity of the SRR film, respectively. The calculated thickness dependent effective resistance of the Pb SRR is shown in Fig. 3(b).

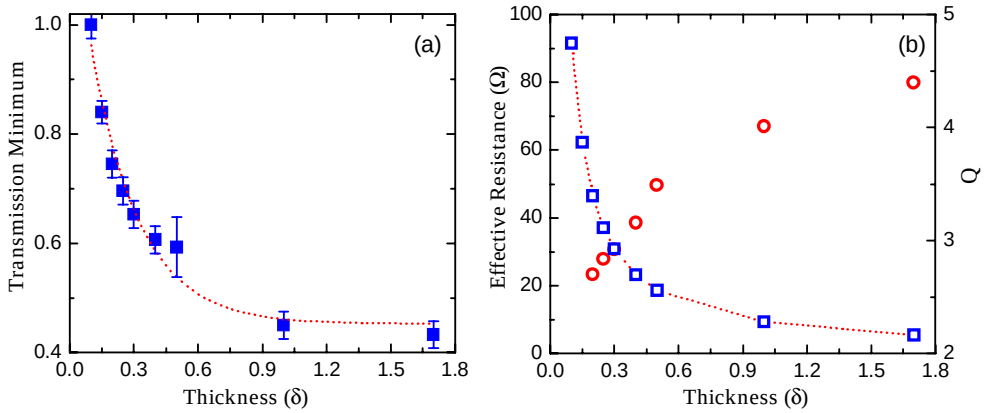

Fig. 3. (a). Transmission minimum at the LC resonance as a function of the SRR thickness in skin depth. (b) Calculated effective resistance of the Pb SRR metamaterials as a function of the metal thickness by use of the equivalent ring model (Squares) and the Quality factor of the Pb metamaterials extracted from the measured transmission spectra as a function of thickness in skin depth (circles). The dotted curves are guides to the eye.

Continuing the treatment of the SRR as an equivalent RLC circuit the resonance enhancement is seen to result from the increase in circulating current due to a decrease in the effective SRR resistance R. Physically, this correlates to the SRR film getting thicker. For the 0.1δ-thick SRRs, the effective resistance of a double SRR unit is 91.5 Ω and there is not sufficient current excited in the SRR to support the LC resonance. However, with a decreased resistance to 62.2 Ω, the 0.15δ-thick SRRs begin to exhibit resonance features. Thus, 0.15δ becomes the critical thickness of the Pb SRRs required to facilitate the emergence of the LC resonance. Finally, for thicker SRRs the resonance strengthens and then gradually saturates as the SRR effective resistance reaches its minimum constant value at 2.0δ thickness.

The effective resistance follows a 1/h functional form that is similar to the behavior of the resonance transmission minimum, shown in Fig. 3(a). In using RLC circuits to model wave propagation through metamaterials the functional dependence of the transmission is dependent on the overall surface impedance [21], which incorporates several effects in addition to ring resistance R, such as substrate permittivity, ring density, and other factors. Therefore, the evolution of the transmission minimum is not expected to exactly follow a 1/h form. Also, the aforementioned formula used for calculating R assumes that the metal conductivity is thickness independent, which is not necessarily true [22-24]. Nevertheless, the data indicate that the sub-skin-depth metals are basically acting as distributed resistors impeding current flow but causing few other changes in the resonant behavior of the ring. The slight resonance shifts that develop with increasing metal thickness do not necessarily indicate

#94061 - $15.00 USD Received 19 Mar 2008; revised 21 Apr 2008; accepted 21 Apr 2008; published 23 Apr 2008

an evolution in the capacitance or inductance of the SRRs, but rather may be the result of coupling between resonant modes of the individual rings. As current flow increases in the SRRs, this coupling strengthens along with the individual resonances, causing some reshaping and frequency shifting.

Another related effect observed in the data is the thickness dependent behavior of the quality (Q) factor of the LC resonance. The Q is a measure of the sharpness of a resonance as defined by the central resonance frequency divided by the measured 3dB power bandwidth, $f_0/\Delta f_{3dB}$. As shown in Fig. 3(b), the measured Q of the SRR LC resonance is improved with increasing metal thickness.

It is worth noting, although from the data we observe that the dipole mode at 1.6 THz begins to develop just as it did at 0.5 THz, the 0.15 skin depth criterion for the LC resonance is not necessarily applicable across the spectrum. This is because the higher-order modes do not share the same current profiles as the LC mode. In fact, dipole currents are largely restricted to the side arms parallel to the terahertz electric field, whereas LC currents oscillate around the entirety of the ring. In other words, one cannot assume a constant current distribution throughout the ring for anything but the LC resonance [20]. Thus the resistance formula may not be valid for higher-order resonances. For this reason we need not expect damping behavior to be the same for LC and higher resonances.

3.2 Simulation

Simulations using CST Microwave Studio were carried out to model the sub-skin-depth resonators [25]. Modeling the Pb films as lossy metals did not produce results that agreed with the experiments. This is because Microwave Studio does not solve Maxwell's equations inside metallic geometries, instead setting up Leontovich boundary conditions on the metal surface. As a result, metallic inclusions of any thickness appear thicker than a skin depth. Therefore, the software was forced to treat the Pb layers as dielectrics having very high permittivity and conductivity (σ = 4.5 × 10^6 $\Omega^{-1}m^{-1}$, ε = –1800). As shown in Fig. 2(b), this resulted in reasonably good agreement with the experimental data capturing most of the measured behavior, including the slight frequency shifting of the resonance with increasing metal thickness. The simulations not only elucidate the nature of many of the features in the data, such as the onset of various higher-order modes (1.8 THz, 2.54 THz), but also reveal additional information. For example, the simulated transmission minimums follow a very uniform decrease with increasing metal thickness, more so than in the measurements. This reveals a possible experimental variation in the Pb conductivity with thickness or a tolerance in the deposited thickness. Such variations are not altogether unexpected in sub skin-depth layers of metals due to non-uniform or non-crystalline growth. In addition, we notice some discrepancies between the data and simulation, particularly in the transmission of the 0.1δ-thick SRRs. This is due partly to the experimental variations discussed above but also the limited resolution and computational accuracy of Microwave Studio in the simulation of very thin metal resonators. Further studies are also being pursued to discover the nature of unique features such as the one at 0.6 THz in which the thickness of the metal seems to have no effect on transmission.

4. Summary

We have experimentally demonstrated optically thin metamaterials resonating in the terahertz regime. The thickness dependent resonance evolution characterized by THz-TDS has shown that remarkable electromagnetic resonances can be developed in planar metamaterials of sub-skin-depth thicknesses. In particular, nearly 70% of the maximum resonance amplitude was achieved in the half-skin-depth thick Pb SRR array. Similar resonance behavior was also observed in optically thin metamaterials made from Ag and Al. The sub-skin-depth approach enables the control and modification of resonance magnitude of a fixed metamaterial design and will benefit applications in integrated subwavelength terahertz components.

#94061 - $15.00 USD Received 19 Mar 2008; revised 21 Apr 2008; accepted 21 Apr 2008; published 23 Apr 2008

Acknowledgments

The authors acknowledge valuable discussions with A. K. Azad. The Oklahoma State team is supported by the National Science Foundation. The Los Alamos contributors gratefully acknowledge the support of the U.S. Department of Energy through the LANL/LDRD Program for this work. This work was performed, in part, at the Center for Integrated Nanotechnologies, a U.S. Department of Energy, Office of Basic Energy Sciences nanoscale science research center jointly operated by Los Alamos and Sandia National Laboratories.

#94061 - $15.00 USD Received 19 Mar 2008; revised 21 Apr 2008; accepted 21 Apr 2008; published 23 Apr 2008